

# Complex Terminating Impedance for AW Filters: the Key for Power Amplifier Co-design

Patricia Silveira, Ángel Triano, Jordi Verdú, and Pedro de Paco  
Universitat Autònoma de Barcelona (UAB)  
Telecommunications and Systems Engineering Department

**Abstract**—Acoustic wave (AW) filters connected to non-50  $\Omega$  system impedance can be a suitable solution for reducing RF front-end module complexity. This paper addresses a general synthesis methodology of acoustic wave ladder filters with complex source and/or load terminations based on electrical parameter extraction procedure of an inline topology using non-resonating nodes. Using a commercial GaN transistor a co-designed PA-AW filter module was simulated providing the expected Chebyshev filter behaviour while keeping excellent PA performance in the passband. Some considerations about the influence of the complex terminations on the filter elements values and behaviour are presented.

**Index Terms**—Complex termination, SAW, BAW, Synthesis, Ladder-type filter, Power amplifier.

## I. INTRODUCTION

Front-end modules include filters manufactured with acoustic wave technologies are usually designed considering that the impedance of the input and output port are 50  $\Omega$  and describing the prescribed frequency response when their input and output port are connected to a 50  $\Omega$  system impedance. Nevertheless, when a preceding/succeeding circuit presents a non-50  $\Omega$  output/input impedance it will be required a inter-stage matching network.

More power efficient RF front ends are continuously demanded for 4G LTE and the upcoming 5G. To improve the RF power amplifier efficiency, one can take advantage of a wide variety of techniques which have shown to be effective on enhancing the average PA efficiency, providing longer battery life and a high integration level [1], [2]. However, despite the effort made to improve the efficiency, the designers typically use input/output matching networks with lumped passive components and also off-chip elements like baluns to deliver power to a 50  $\Omega$  load [3]–[5]. These elements introduce losses, increasing the complexity design and reducing the final PA figures.

Instead of cascading PA and filter a co-design technique assists the designer to remove the commonly employed output-matching network (OMN) after the transistor, achieving a lower circuit complexity and leading to a higher efficiency [6]. Fig. 1 shows the conventional cascade topology and the co-designed structure.

From the design point of view, acoustic wave technology have stringent constraints to consider: material system, power management capability, self-heating effects, number of different resonant frequencies, size and, nature and allocation of the

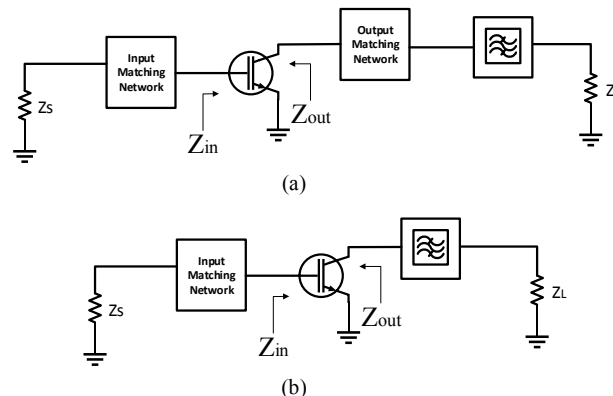


Fig. 1. Power amplifier schematic circuit (a) Conventional topology with OMN and bandpass filter, and (b) Co-designed PA-AW filter.

external elements. Also, it is mandatory the compliance of the spectrum mask specifications. All these requirements should be considered in the design process applying an organized methodology native oriented to accommodate electromechanical coupling constraints.

This paper shows that the filter performance with complex source/load termination impedance is exactly that obtained when a 50  $\Omega$  termination system is assumed. Moreover, the values of the extracted BvD-model elements are properly assimilated by the AW technology under consideration, what makes its manufacture feasible in general. Considering a PA with a frequency-dependent output impedance loading the filter causes a minor deviation in the bandpass filter response, but maintaining good figures and excellent agreement for the PA-AW filter module.

## II. COMPLEX SOURCE/LOAD FILTER SYNTHESIS THEORY

Despite previous AW filter synthesis works deal with real source and load impedance terminations [7], [8], the analysis may be generalized to networks with complex impedance terminations. An AW ladder-type filter where the number of resonators ( $N$ ) is equal to the prescribed transmission zeros (TZ), leading to a fully canonical filter, can be realized with a generalized Chebyshev filtering function. The characteristic polynomials are generated through an efficient recursive technique, obtaining  $E(s)$ ,  $F(s)$  and  $P(s)$  polynomials and the normalization constants  $\epsilon$  and  $\epsilon_R$  [9]. These polynomials are

turned into an electrical circuit prototype using a synthesis approach based on the [ABCD] transfer matrix.

The  $F(s)$  polynomial is affected by a phase term in (1) that has not effect on the return and insertion losses of the filter since the argument  $\phi_{11}$  is a real quantity [10]. However, this phase shift is important to allow the extraction of the first/last transmission zero without extra reactive elements at the input and/or output ports or for the proper design of duplexers and multiplexers [11]. In this work is also proved that the input phase  $\phi_{11}$  plays a very important role in order to obtain an AW network matched to different source impedance values with a single tuning element, the input external reactive element.

$$F(s) = e^{j\phi_{11}} F(s) \quad (1)$$

For a two-port network the [ABCD] matrix is built as follows:

$$[ABCD] = \frac{1}{jP(s)/\varepsilon} \begin{bmatrix} A_n(s) & B_n(s) \\ C_n(s) & D_n(s) \end{bmatrix} \quad (2)$$

If the network is operating between complex source and load impedances  $Z_S$  and  $Z_L$ , then the [ABCD] matrix polynomials are related to them and the characteristic polynomials as [9]:

$$\begin{aligned} A_n(s) &= \frac{1}{2} [(Z_S^* E(s) + Z_S F(s)/\varepsilon_R) - (-1)^N (Z_S^* E(s) + Z_S F(s)/\varepsilon_R)^*] \\ B_n(s) &= \frac{1}{2} [Z_L^* (Z_S^* E(s) + Z_S F(s)/\varepsilon_R) + (-1)^N Z_L (Z_S^* E(s) + Z_S F(s)/\varepsilon_R)^*] \\ C_n(s) &= \frac{1}{2} [(E(s) - F(s)/\varepsilon_R) + (-1)^N (E(s) - F(s)/\varepsilon_R)^*] \\ D_n(s) &= \frac{1}{2} [Z_L^* (E(s) - F(s)/\varepsilon_R) - (-1)^N Z_L (E(s) - F(s)/\varepsilon_R)^*] \\ P(s) &= P(s) \sqrt{(R_S R_L)} \end{aligned} \quad (3)$$

where  $R_S$  and  $R_L$  represent the real part of the source and load impedances respectively.

The synthesis of the filter is carried out by means of successive extractions from the [ABCD] matrix polynomial since the ladder-type AW filter is composed by Non-Resonant Nodes (NRN) with dangling resonators separated by unitary admittance inverters ( $J$ ) as its is shown in Fig. 2. The extraction technique is the same as the stand-alone filter when  $Z_S=Z_L=50 \Omega$  since the [ABCD] matrix has been re-normalized with respect to another reference impedance different from  $50 \Omega$ .

Finally, the two-port S-parameter matrix is reformulated in terms of the known termination impedance and the [ABCD] polynomials as follows [12]:

$$S_{11}(s) = \frac{A(s)Z_L + B(s) - C(s)Z_S^*Z_L - D(s)Z_S^*}{A(s)Z_L + B(s) + C(s)Z_S Z_L + D(s)Z_S}$$

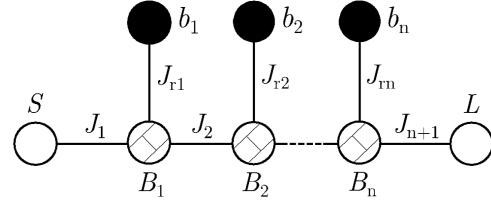


Fig. 2. Nodal diagram of a low-pass AW ladder-type filter.

$$\begin{aligned} S_{12}(s) &= \frac{2(A(s)D(s) - B(s)C(s))\sqrt{(R_S R_L)}}{A(s)Z_L + B(s) + C(s)Z_S Z_L + D(s)Z_S} \\ S_{21}(s) &= \frac{2\sqrt{(R_S R_L)}}{A(s)Z_L + B(s) + C(s)Z_S Z_L + D(s)Z_S} \\ S_{22}(s) &= \frac{-A(s)Z_L^* + B(s) - C(s)Z_S Z_L^* + D(s)Z_S}{A(s)Z_L + B(s) + C(s)Z_S Z_L + D(s)Z_S} \end{aligned} \quad (4)$$

### III. PA-AW FILTER CO-DESIGN

In order to demonstrate the PA-AW filter co-design concept and having into account the technological feasibility of the AW filter, a 4W GaN transistor Cree CGH40006P up to 6 GHz was selected as the RF power device. The filter was designed to address sub-band 41 at 2.605 GHz with a BW=60 MHz. Despite de lack of commercial high power AW filter, one can find some reference examples in the market like the BAW filter from Qorvo QPQ1300.

According to the data provided by the manufacturer, the values chosen for the transistor bias network are  $V_{GS}=-2.9$  V,  $V_{DS}=27$  V and  $I_{DS}=125$  mA to achieve a class AB amplifier. It is also necessary to introduce a series parallel RC network to ensure the stability of the amplifier before the DC block in the gate with  $R=10 \Omega$  and  $C=2$  pF.

For the transistor characterization the source/load-pull simulations were carried out with Agilent's Advanced Design System (ADS) setup. The source/load-pull simulations provide the optimum source/load impedances for maximum power-added efficiency (PAE) and maximum output power which were used for designing the input matching network (IMN) and the filter as an OMN of the PA. The optimum source/load transistor impedances for this design  $Z_{SPA} = 11.5 + 13.5j \Omega$  and  $Z_{LPA} = 16.53 + 42.87j \Omega$  were selected to achieve a PAE = 52% and  $P_{out} = 35.2$  dBm. Our main concern has been validate filter response integrity so amplifier figures can be improved by using different techniques out of the scope of this work.

The IMN was implemented with an RL network matched at the central frequency. For the OMN, a 5th-order AW filter was synthesized with a complex source impedance  $Z_{SF} = Z_{LPA}^* = 16.53 - 42.87j \Omega$  following the extraction procedure described in [7] and applying (3). The filter output impedance is  $Z_{LF} = 50 \Omega$ .

Having into account the filter specifications (spectrum mask) for this sub-band 41 and in order to fit with an effective electromechanical coupling constant  $k_{eff}^2 = 8.76\%$  in all resonators and also fulfill the technological bounds of the static capacitance of the filter ( $C_0$ ) in each resonator, the synthesis

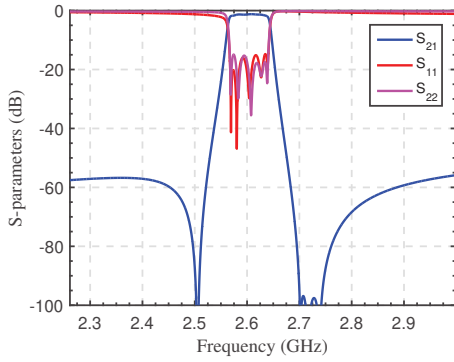


Fig. 3. S-parameters filter response with  $Z_S = 16.53-42.87j \Omega$  and  $Z_L = 50 \Omega$ .

TABLE I

BANDPASS ELEMENTS OF THE FILTER OBTAINED FROM THE BVD MODEL

$f_s$ [GHz]	$k_{eff}^2$ [%]	$C_0$ [pF]	$C_a$ [pF]	$L_a$ [nH]
2.64	8.76	0.2875	0.0221	164.54
2.50	8.76	5.3436	0.4110	9.81
2.60	8.76	0.3101	0.0238	156.61
2.50	8.76	5.2836	0.4064	9.92
2.62	8.76	0.4119	0.0317	116.65

procedure through an automatic search engine was performed. The following configuration was obtained:

- Normalized transmission zeros  $\Omega_z$  (rad/s):  
{3.82, -2.84, 2.72, -2.84, 3.14 }
- RL (dB): 15.3
- $\phi_{11}$ ( $^\circ$ ): -133.5

The circuit elements of the lowpass nodal representation depicted in Fig. 2 were obtained:  $B_1=-4.3691$ ,  $B_2= 4.7224$ ,  $B_3= -3.9412$ ,  $B_4 = 4.6687$ ,  $B_5 = -3.0002$ ,  $J_{r1}= 3.5401$ ,  $J_{r2}= 3.5914$ ,  $J_{r3}= 3.2727$ ,  $J_{r4}= 3.5706$ ,  $J_{r5}= 2.8821$ , and  $b_i=-\Omega_z$ . The inverters between NRNs are unitary with an alternating sign, and the input/output external elements are  $B_S = -1.6164$  and  $B_L = -0.5450$  respectively.

The calculated lowpass elements are transformed in frequency with an impedance denormalization to obtain the BVD equivalent circuit. It is well-known that the Butterworth-van Dyke (BVD) model offers a faithful representation of the electrical performance for piezoelectric resonators in the main resonance vicinity with the system losses included. Table I resumes the BVD element values extracted from the network. For this example, and related to the calculated input phase  $\phi_{11}$ , the external elements are two input/output inductors  $L_S = 1.89$  nH and  $L_L = 5.60$  nH respectively. S-parameters response of the filter calculated with (4) is shown in Fig. 3 considering a series and parallel quality factor  $Q=1500$ . In the selected topology, the first resonator is series, so the external element would be in shunt position.

With the defined elements of the IMN and OMN, the co-design PA is now complete. Simulation of the entire circuit schematic is performed using the harmonic-balance (HB) simulator in ADS. Fig. 4 shows the simulated large signal S-

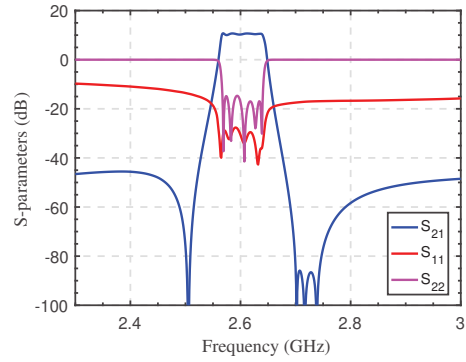


Fig. 4. Large signal S-parameters response for  $P_{in}=25$  dBm.

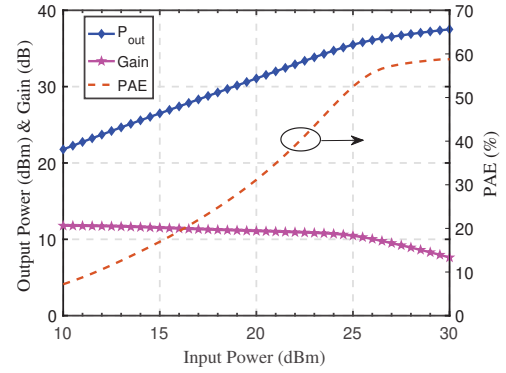


Fig. 5. Simulated PA-AW module performance with ideal elements vs input power at 2.605 GHz

parameters from 2.7 to 3.0 GHz with a constant 25-dBm input power. The  $S_{11}$  shape evidences that the filter is completely isolated by the transistor seen from the input port.

Fig. 5 shows the simulated output power, efficiency and gain across the input power range from 10 to 30 dBm at the center frequency of 2.605 GHz, indicating a 35.5-dBm output power, a PAE= 52.5% and Gain=10.466 dB under 25-dBm input stimulus.

In order to evaluate the performance of the filter and its response degradation when preceded by the amplifier, a simulated comparison between the stand-alone filter response adding the PA gain and the co-designed module was implemented considering lossy elements. Both responses show a good agreement as depicted in Fig. 6, but some differences appears in the passband.

In the case of stand-alone filter, the synthesis is carried through considering a frequency-independent complex source termination, so  $Z_{SF}$  is constant in the entire frequency range. Meanwhile, the PA output impedance is frequency dependent and the PA gain presents a slight negative slope affecting the whole performance, but of course in both cases. Consequently, a non equiripple response with 0.4 dB is observed in this example. In any case it is an excellent starting point for further optimizations.

#### IV. CONSIDERATIONS

In case of the synthesis of fully canonical in-line topology, where AW ladder topology belongs, has been observed that the

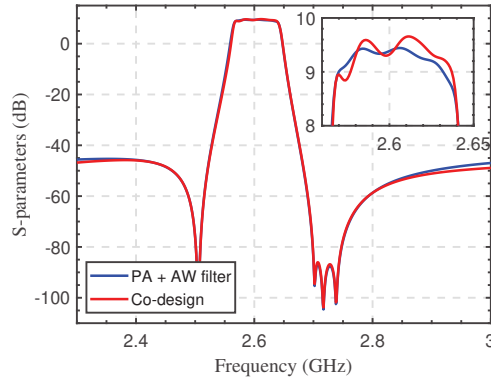


Fig. 6. Simulated comparison between the stand-alone filter response adding the PA gain and the co-designed module.

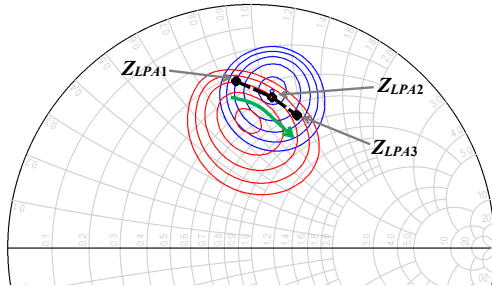


Fig. 7.  $Z_{LPA}$  locus with the variation of the input reactive element  $L_S$ . PAE (blue) and Output power (red) contours from the load-pull simulation of the CGH40006 GaN transistor at 2.605 GHz.

variation of  $Z_S$  and/or  $Z_L$ , maintaining the same transmission zeros, affects the static capacitance of all resonators of the filter  $C_0$ , but only the capacitance ratio (r-factor) and series resonant frequency of the first and last resonators. However, it can be highlighted that exist a family of source impedances  $Z_S$  with constant conductance that are matched with the complex input impedance of one filter varying only the value of the input shunt reactive element.

As was mentioned before, input phase  $\phi_{11}$  controls the value of the input reactive element, therefore, we can synthesize a filter for a given  $Z_{S1}$  with InputPhase1 and the same filter will be matched to  $Z_{S2}$  with InputPhase2 if  $Z_{S1}$  and  $Z_{S2}$  have the same conductance. The input external element is the only element that will change.

Using the example presented in the previous section, changing the values of  $\phi_{11}$  in the synthesis procedure to:  $\phi_{11,2} = -143.9^\circ$  and  $\phi_{11,3} = -154.5^\circ$  we obtain a filter matched to a PA with  $Z_{LPA2} = 25 + 50.7j \Omega$  and  $Z_{LPA3} = 35 + 56.9j \Omega$  obtaining an input external element  $L_{S2} = 2.19$  nH and  $L_{S3} = 2.47$  nH respectively with the same BvD AW elements showed in Table I, including the output reactive element. The load transistor impedances  $Z_{LPA1}$ ,  $Z_{LPA2}$  and  $Z_{LPA3}$  have the same conductance  $G = 0.0078 S$ . The position of  $Z_{LPA}$  mentioned above is represented in Fig. 7 where the contours resulting from the load-pull simulation of PAE and output power calculated at the fundamental frequency 2.605 GHz with  $P_{in} = 25$  dBm are shown. The figure point out the

displacement of  $Z_{LPA}$  round a constant conductance circle reached by having a single tuning element in order to match the filter with different impedance by tuning only  $L_S$  (green trace) while the PA performance can be properly tuned.

## V. CONCLUSIONS

This work presents a synthesis methodology of acoustic ladder filters based on electrical parameter extraction procedure of an inline topology using non-resonating nodes generalized to networks with complex impedance terminations. The spectrum fulfillment and the technological accommodation constraints of micro-acoustics technologies have been taken into account in order to obtain a complete solution. A co-designed approach was implemented achieving a good performance in the design of the PA and filter building blocks. The assumption of a frequency independent complex source termination as a good starting point was verified. Moreover, was addressed the tunability of the input reactive element in order to match the same filter to different complex source impedances, giving the designer a degree of freedom for filter adjustment.

## ACKNOWLEDGMENT

The authors would like to thank to Cree Inc., Durham, NC, USA, for supplying the transistor model.

## REFERENCES

- [1] F. Wang, D. Kimball, J. Popp, A. Yang, D. Y. C. Lie, P. Asbeck, and L. Larson, "Wideband envelope elimination and restoration power amplifier with high efficiency wideband envelope amplifier for wlan 802.11g applications," in *IEEE MTT-S Int. Microw. Symp.*, 2005., June 2005, pp. 4 pp.-648.
- [2] Y. Li, J. Lopez, P. Wu, W. Hu, R. Wu, and D. Y. C. Lie, "A sige envelope-tracking power amplifier with an integrated cmos envelope modulator for mobile wimax/3gpp lte transmitters," *IEEE Trans. Microw. Theory Techn.*, vol. 59, no. 10, pp. 2525–2536, Oct 2011.
- [3] R. Wu, Y. Liu, J. Lopez, C. Schecht, Y. Li, and D. Y. C. Lie, "High-efficiency silicon-based envelope-tracking power amplifier design with envelope shaping for broadband wireless applications," *IEEE J. Solid-State Circuits*, vol. 48, no. 9, pp. 2030–2040, Sep. 2013.
- [4] B. Francois and P. Reynaert, "A fully integrated watt-level linear 900-mhz cmos rf power amplifier for lte-applications," *IEEE Trans. Microw. Theory Techn.*, vol. 60, no. 6, pp. 1878–1885, June 2012.
- [5] M. Gilasgar, A. Barlab'e, and L. Pradell, "A 2.4 ghz cmos class-f power amplifier with reconfigurable load-impedance matching," *IEEE Trans. Circuits Syst. I: Regular Papers*, vol. 66, no. 1, pp. 31–42, Jan 2019.
- [6] K. Chen, J. Lee, W. J. Chappell, and D. Peroulis, "Co-design of highly efficient power amplifier and high- $q$  output bandpass filter," *IEEE Trans. Microw. Theory Techn.*, vol. 61, no. 11, pp. 3940–3950, Nov 2013.
- [7] J. Verdú, I. Evdokimova, P. de Paco, T. Bauer, and K. Wagner, "Systematic synthesis methodology for the design of acoustic wave stand-alone ladder filters, duplexers and multiplexers," in *2017 IEEE Int. Ultrason. Symp. (IUS)*, Sep. 2017.
- [8] A. Giménez, J. Verdú, and P. de Paco Sánchez, "General synthesis methodology for the design of acoustic wave ladder filters and duplexers," *IEEE Access*, vol. 6, pp. 47 969–47 979, 2018.
- [9] R. J. Cameron, C. M. Kudsia, and R. R. Mansour, *Microwave filters for communications systems: fundamentals, design, and applications*. Wiley, 2018.
- [10] S. Amari and G. Macchiarella, "Synthesis of inline filters with arbitrarily placed attenuation poles by using nonresonating nodes," *IEEE Trans. Microw. Theory Techn.*, vol. 53, no. 10, pp. 3075–3081, Oct 2005.
- [11] P. Silveira, J. Verdú, and P. de Paco, "Star-junction multiplexer design under minimum susceptance networks approach," in *2019 IEEE MTT-S Int. Microw. Symp - IMS*, June 2019.
- [12] D. A. Frickey, "Conversions between s, z, y, h, abcd, and t parameters which are valid for complex source and load impedances," *IEEE Trans. Microw. Theory Techn.*, vol. 42, no. 2, pp. 205–211, Feb 1994.